

Benthic Megafaunal Community Structure  
and Biodiversity Along a Sea Ice Gradient  
on the Western Antarctic Peninsula:  
Insights into Climate Warming

A THESIS SUBMITTED TO  
THE GLOBAL ENVIRONMENTAL SCIENCE  
UNDERGRADUATE DIVISION IN PARTIAL FULFILLMENT  
OF THE REQUIREMENTS FOR THE DEGREE OF

BACHELOR OF SCIENCE

IN

GLOBAL ENVIRONMENTAL SCIENCE

AUGUST 2010

By

Christian E. Clark

Thesis Advisors

Craig R. Smith

Laura Grange

We certify that we have read this thesis and that, in our opinion, it is satisfactory in scope and quality as a thesis for the degree of Bachelor of Science in Global Environmental Science.

THESIS ADVISORS

---

Craig R. Smith  
Department of Oceanography

---

Laura Grange  
Department of Oceanography

## ACKNOWLEDGMENTS

I would like to acknowledge the National Science Foundation for funding, the captain and crew of the AS/RV Laurence M. Gould and RV/IB Nathaniel B. Palmer, the United States Antarctic Program and Raytheon Polar Services for help with logistical support and sample collection, everyone from North Carolina State University for their help with sample collection and ship morale, my advisors Craig R. Smith and Laura Grange, all members of the Smith Laboratory, Rhian Waller for help with species identification, and the entire Global Environmental Science family: Jane Schoonmaker, Rene Tada, Nancy Koike, Leona Anthony, and classmates.

## ABSTRACT

The Western Antarctic Peninsula (WAP) is experiencing some of the fastest rates of regional warming in the world, resulting in the collapse of ice shelves, warming ocean temperatures, and increased melt and retreat of glaciers. Winter sea ice coverage in the waters off the WAP has decreased in duration and extent over the last half century. The significant changes observed off the WAP are extremely important in studying the effects that global climate change may have on marine ecosystems. Observed changes in sea ice may have negative effects on benthic ecosystems due to interactions between sea ice, primary production, and pelagic-benthic coupling. The effects of sea ice duration on deep benthic community structure (550-650 m depth) along the WAP continental shelf are not well understood. We evaluated megafaunal abundance, species richness, and community structure at five physically similar midshelf stations along a strong latitudinal sea ice gradient from Smith Island (63S) to Marguerite Bay (68S). Data collection included replicate towed “Yoyo Camera” transects (i.e. quantitative photographic surveys) of the seafloor at each station. Our most northern station (Sta. AA) experiences ~1 month of sea ice per year and our most southern station (Sta. G) sees >7 months of sea ice cover per year. This study found that both megafaunal abundance and community structure varied latitudinally along our north-south transect on the WAP in concert with sea ice duration. Interestingly, species richness showed no general patterns or trends as a result of sea ice extent. These results suggest that sea ice

loss is likely to alter megabenthic community structure on the WAP, possibly causing a shift from deposit-feeder dominated to suspension-feeder dominated communities along the southern WAP.

# TABLE OF CONTENTS

Acknowledgments.....	iii
Abstract.....	iv
List of Tables.....	viii
List of Figures.....	ix
List of Abbreviations.....	x
Chapter 1: Introduction.....	1
1.1. Climate Change in Antarctica.....	1
1.2. Benthic-pelagic Coupling.....	2
1.3. Labile Organic Matter Food Bank.....	3
1.4. WAP Benthic Megafaunal Abundance, Species Richness, and Community Structure.....	4
Chapter 2: Methods and Materials.....	7
2.1. Experimental Design.....	7
2.2. Photographic Survey Methods.....	9
2.3. Data Processing.....	12
2.4. Statistical Analysis.....	14
Chapter 3: Results.....	15
3.1. Abundance.....	15
3.1.1. Mean Abundance per m <sup>2</sup> .....	15
3.1.2. Statistical Results for Abundance.....	16

3.1.3. Most Abundant Species.....	18
3.2. Species Diversity.....	20
3.2.1. Species Richness and Accumulation.....	20
3.2.2. Evenness and Rarefaction.....	24
3.3. Community Composition.....	26
3.3.1. Community Structure between Transects and Stations.....	26
3.3.2. Functional Groups.....	28
Chapter 4: Discussion.....	30
4.1. Abundance.....	30
4.2. Species Richness.....	33
4.3. Community Composition and Trophic Structure.....	37
4.4. Conclusion.....	39
Appendix.....	40
References.....	43

# LIST OF TABLES

<u>Table</u>	<u>Page Number</u>
Table 2.1: Table of Number of Images Analyzed for each CRS# and Station.....	13
Table 3.1: Mean Abundance per m <sup>2</sup> .....	15
Table 3.2: P-values for Mann-Whitney Test of Abundances.....	17
Table 3.3: Top 10 Most Dominant Species at each Station.....	19

## LIST OF FIGURES

<u>Figure</u>	<u>Page Number</u>
Figure 2.1: Map of Sampling Stations along the WAP.....	8
Figure 2.2: Mean Annual Sea Ice Cover for each Station.....	9
Figure 2.3: Yoyo Camera.....	10
Figure 3.1: Mean Abundances per m <sup>2</sup> .....	16
Figure 3.2: Species Accumulation Curves, Station AA.....	21
Figure 3.3: Species Accumulation Curves, Station B.....	21
Figure 3.4: Species Accumulation Curves, Station E.....	22
Figure 3.5: Species Accumulation Curves, Station F.....	22
Figure 3.6: Species Accumulation Curves, Station G.....	23
Figure 3.7: Chao 1 Estimator.....	24
Figure 3.8: Rarefaction by Station.....	25
Figure 3.9: Evenness for each Station.....	26
Figure 3.10: FB-2 Megafaunal Structure MDS Plot.....	27
Figure 3.11: Bray-Curtis Transect Similarity.....	28
Figure 3.12: Functional Group Composition by Station.....	29

## LIST OF ABBREVIATIONS

WAP:	Western Antarctic Peninsula
K:	Kelvin
AASW:	Antarctic Surface Waters
ACC:	Antarctic Circumpolar Current
CDW:	Circumpolar Deep Water
POM:	Particulate Organic Matter
POC:	Particulate Organic Carbon
°C:	Degrees Celsius
Chl a:	Chlorophyll a
S:	South
m:	Meter
FOODBANCS:	Food for the Benthos on the Antarctic Continental Shelf
FB-2-1:	FOODBANCS 2 Cruise 1
FB-2-2:	FOODBANCS 2 Cruise 2
FB-2-3:	FOODBANCS 2 Cruise 3
AS/RV-LMG:	Antarctic Supply and Research Vessel Laurence M. Gould
RV/IB-NBP:	Research Vessel Ice Breaker Nathaniel B. Palmer
mm:	millimeter
cm:	Centimeters
CRS#:	CRS Number – unique deployment number

m <sup>2</sup> :	Meters squared
s:	Second
km:	Kilometer
TIFF:	Tagged Image File Format
Sta.:	Station
Stas.:	Stations
v.:	Version
sp.:	Species
UGE:	Ugland Curve
Es:	Expected species
nMDS:	Nonmetric Multidimensional 4 <sup>th</sup> Root Scaling plot
m/so:	Mobile, Suspension Feeder
s/so:	Sessile, Scavenger/Omnivore
m/sf:	Mobile, Suspension Feeder
s/sf:	Sessile, Suspension Feeder
m/df:	Mobile, Deposit Feeder
s/df:	Sessile, Suspension Feeder
m/c:	Mobile, Carnivore

# CHAPTER 1: INTRODUCTION

## 1.1. Climate Change in Antarctica

The Antarctic Peninsula is experiencing some of the fastest rates of regional warming in the world and it is resulting in the collapse of ice shelves, warming ocean temperatures, and the increased melt and retreat of glaciers (Clarke et al. 2007). This rapid regional warming of the Antarctic Peninsula has resulted in the loss of at least seven major ice shelves in the last 50 years (Vaughn and Doake 1996). Accompanying these ice shelf collapses is decreased winter sea ice coverage. Regional winter sea ice coverage in the Bellingshausen and Amundsen seas, off the Western Antarctic Peninsula (WAP), has decreased in seasonal duration and in extent by almost 10% per decade for the last 50 years (Clarke et al. 2007). Subsequently in each of these two areas the mean annual air temperature has increased by 1.5 K in the same period of time, compared to a global increase of 0.6 K (Clarke et al. 2007).

The significant changes observed off the WAP are extremely important in studying the effects that global climate change may have on marine ecosystems and major earth systems. The WAP is the only area of Antarctica to show such a significant decrease in seasonal sea ice extent and duration (Clarke et al. 2007). The trend of decreased sea ice coverage and duration in the seas off the WAP may have negative effects on marine and benthic ecosystems due to the unique interactions of the benthic and pelagic environments on the Antarctic continental shelf.

There are three characteristics of the Antarctic Surface Waters (AASW) of the WAP that are responsible for the unique coupling of environments: exchange with the atmosphere, sea ice coverage and duration, and interaction with the Antarctic Circumpolar Current (ACC) carrying Circumpolar Deep Water (CDW) (Smith & Klinck 2002). The Antarctic continental shelf is remarkably deep compared to most continental shelves. For most continental shelves the shelf is located within, or close to, the depth of the seasonal mixed layer, which is not the case for the Antarctic continental shelf (Clarke et al. 2007). This is a unique situation and as a result most of the continental shelf is located below the depth of AASW. The fact that the continental shelf is located so deep is important since it is suggested that the deep water of the ACC is warming much faster than the mean rate calculated for the global ocean (Barnet et al. 2005, Clarke et al. 2007). Increased warming could have significant impacts on marine ecosystems and their ability to cycle nutrients.

## **1.2. Benthic-pelagic Coupling**

All of the different variables associated with the WAP lead to an interesting benthic-pelagic ecosystem on the continental shelf. The benthic-pelagic coupling discussed in this paper will mainly focus on the downward coupling, in which the water-column processes exert control on the benthos. There is a great deal of evidence that suggests that benthic-pelagic coupling can considerably influence material cycles, community dynamics, and fisheries yields in shelf ecosystems (Smith et al. 2006). Benthic-pelagic coupling is accomplished off the WAP by seasonal fluxes of particulate

organic matter (POM) raining down through the water-column providing food for key components of the benthic food web, such as suspension feeders, deposit feeders, and sediment microbes (Smith et al. 2006).

The environmental properties of the WAP shelf ecosystem determine the seasonal variation of these POM fluxes to the benthic environment. These properties include: summer and winter variations in sunlight, seasonal sea ice cover and its duration, and water-column stratification. Taken together, these properties support development of strong seasonality in pelagic primary production in Antarctica (Smith et al. 2006). Seasonal variation in primary production causes distinct summer phytoplankton blooms, which may cause higher export ratios and mass settling of phytoplankton to the benthos during the summer season (Smith et al. 2006). Sinking and settling of organic material to the shelf floor allows for the development of benthic communities. The composition and size of benthic communities reflect the production processes of the waters above, and can yield important insights into the climate-driven changes of coastal pelagic ecosystems.

### **1.3. Labile Organic Matter Food Bank**

The highly climate-driven seasonal flux of particulate organic carbon (POC) to the WAP shelf during the summer bloom allows for a large deposition of labile organic material on shelf sediments, which supports benthic detritivores and microbial assemblages (Mincks et al. 2005). However, despite its labile nature, the consistently low bottom-water temperatures in the WAP (-2.0 to 1.0°C) region may slow the metabolic remineralization of organic material deposited on the shelf floor and allow it to be buried

in the shelf sediments (Mincks et al. 2005, Nedwell 1999).

Mincks et al. (2005) suggested that a combination of increased particle sinking rates and low-temperature inhibition of metabolic activity could cause a build-up and storage of organic material in WAP sediments and lead to a long-term ‘food bank’ in shelf sediments. Due to the large area extent of the Antarctic continental shelf, which covers 11% of the total area of continental shelf worldwide, the ability of WAP sediments to sequester organic carbon in a sediment ‘food bank’ is extremely important in understanding the community structure of benthic megafauna on the seafloor of the deep continental shelf of the WAP (Clarke and Johnston 2003).

#### **1.4. WAP Benthic Megafaunal Abundance, Species Richness, and Community Structure**

The rapid climate change seen along the WAP over the last half-century is expected to continue if not increase in the future. In an area where marine ecosystems are heavily dependent on sea ice extent, duration and seasonal phytoplankton blooms, increased warming will likely play a key role in determining ecosystem structure. This is primarily due to the likelihood for decreased sea ice duration in the coastal waters of the WAP. In the long term, decreases in sea ice will likely cause increases in primary production in the surface waters, due to increased light availability in a light limited environment (e.g., Arrigo et al. 2008). This in turn, will alter the quantity and quality of food availability to the coastal food web and modify phytodetrital rain down to the benthos. These changes in quantity and quality of primary production will vary

temporally and spatially, and are likely to influence long-term stability of the WAP ecosystem.

In a recent study, Montes-Hugo et al. (2009), satellite observations were compiled for Chlorophyll a (Chl a) concentrations in surface waters of the WAP as an indicator of primary production levels. The study found that, when current satellite observations of Chl a were compared to a baseline data set from 1978-1986, primary production levels have indeed changed in the past thirty years (Montes-Hugo et al. 2009). In coastal waters of the northern region of the WAP, primary production levels have dropped considerably since the early 1980's and have increased in surface waters of the southern WAP region (Montes-Hugo et al. 2009). They attributed the decreases in the northern region to highly reduced sea ice seasons where the lack of sea ice has allowed increased turbulent mixing, increased cloudiness, and resulted in deeper mixed layers, thereby decreasing the productivity of the waters by actually decreasing the exposure of primary producers to light (Montes-Hugo et al. 2009). On the other hand, the surface waters of the southern WAP appear to be sustaining greater primary production from shortened sea ice seasons, more light availability, and increased mixing (Montes-Hugo et al. 2009).

Therefore, the relationship between, a reduction of sea ice and primary productivity of the coastal waters may be complicated on shorter time and spatial scales, destabilizing or at least altering WAP food webs (Montes-Hugo et al. 2009). Consequently, changes in primary production along the WAP due to sea ice loss will most likely change the structure of the coastal marine ecosystems. Decreased phytoplankton blooms along the northern WAP appear to have substantially changed the pelagic food

web (Montes-Hugo et al. 2009) and therefore altered food fluxes to the benthos, resulting in less phytodetrital rain down. However, increased primary production along the southern WAP has likely increased the amount of food availability and amplified food fluxes to the benthos. These productivity changes, both positive and negative, are expected to alter community structure from the bottom up.

Due to the central importance of sea ice extent and duration to the WAP ecosystem this study will focus on changes to the benthos along a sea ice gradient along the WAP shelf. The main questions that this study will address are: how does benthic megafaunal abundance, community structure, trophic composition, and diversity vary along a strong latitudinal sea ice gradient on the WAP continental shelf? We hypothesize that megafaunal abundance, community structure and trophic composition, and species biodiversity will vary latitudinally concomitantly with variations in sea ice extent and duration.

## CHAPTER 2: METHODS AND MATERIALS

### 2.1. Experimental Design

In this study we worked at five physically similar mid-shelf stations along the WAP continental shelf from approximately 63° S to 68° S. These stations all consisted of soft sediment bottoms and low current regimes at depths from 550 m to 650 m, allowing us to maintain relatively constant benthic habitat variables along a latitudinal gradient on the WAP continental shelf. Stations were named alphabetically starting with station AA our most northern station, station B, station E, station F, and station G our most southern station located off of Marguerite Bay, as seen in Figure 2.1. This north-south transect partially overlaps stations from a previous study, FOODBANCS, which assessed the benthic community structure along an east-west transect sampling an inner shelf station A, a mid-shelf station B (used also in this project), and an outer-shelf station C.

The orientation of our north-south transect allowed us to sample along a strong sea ice gradient. Srsen et al. (unpublished data), shows that average annual sea ice duration for the period 2004 - 2008 increases from north to south along our transect from a minimum of 1.4 months per year at station AA to a maximum of 7.6 months per year at station G (Figure 2.2). Stations were studied at three time points during two summer cruises (cruises FB-2-1 and FB-2-3) aboard the Antarctic Supply and Research Vessel the Laurence M. Gould (AS/RV-LMG), February to mid March of 2008 and 2009, and one winter cruise (cruise FB-2-2) on the Research Vessel Ice Breaker Nathaniel B. Palmer (RV/IB-NBP), from July to early August of 2009. The cruise schedule allowed us to

sample during both winter and summer for comparisons of the benthic community patterns across seasons and years. This is important when considering the large seasonal differences in nutrient fluxes to the benthos along the WAP, which is characterized by large fluxes during summer months and very little during winter months, as well as high interannual variability (e.g., Smith et al. 2006).

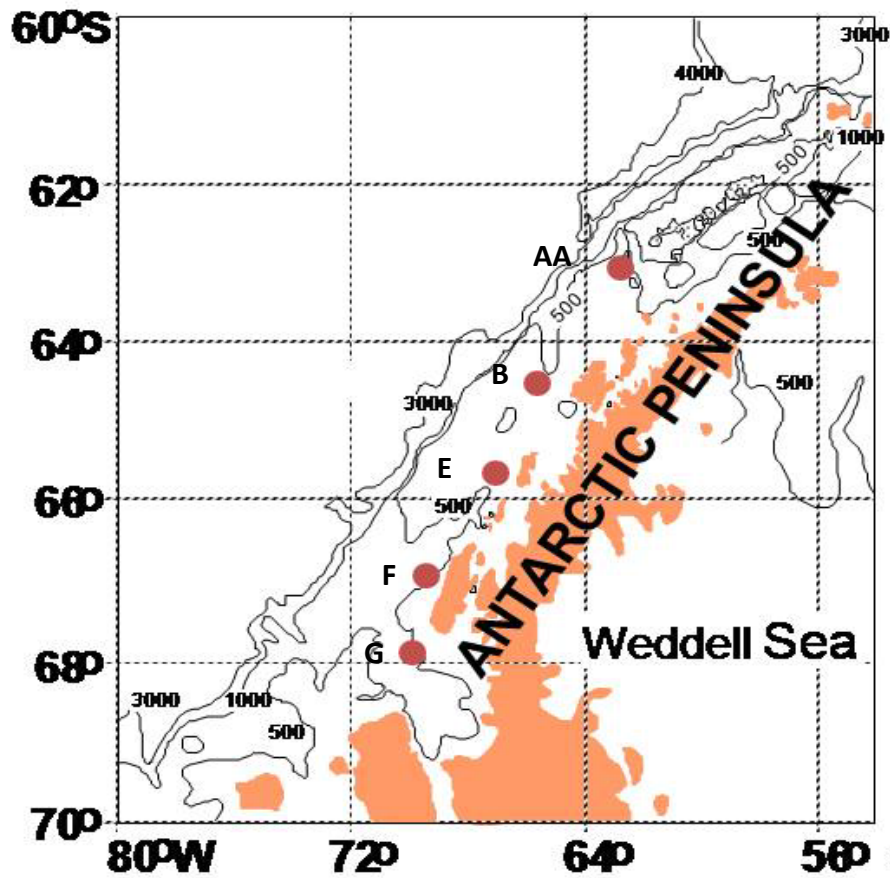


Figure 2.1: Sampling stations AA, B, E, F, and G located along the Western Antarctic Peninsula (from Srsen et al., unpublished). Dots indicate sampling stations and the Antarctic Peninsula is shown in solid color. Lines note 500-meter isobaths.

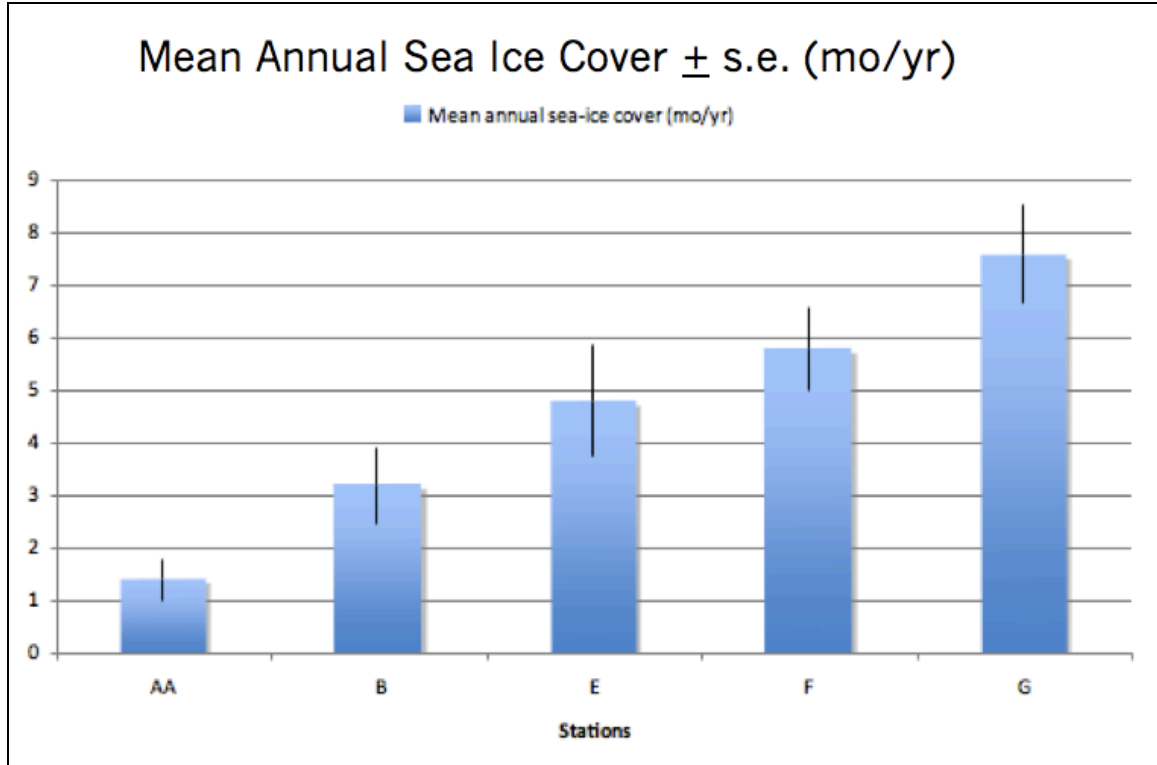


Figure 2.2: Mean annual sea ice cover  $\pm$  standard error. Vertical blue bars indicate months of sea ice cover per year for each of our five sampling stations (AA, B, E, F, and G) based on satellite data from the National Snow and Ice Data Center (Srsen et al., unpublished).

## 2.2. Photographic Survey Methods

Photographic surveys were conducted using a “Yoyo Camera” system developed for the project. This consists of a vertically oriented camera with a strobe one meter away, actuated by a bottom contact switch (Figure 2.3). The camera is an Ocean Imaging Systems DSC 10000 digital still camera in titanium housing, with a 10.2 mega pixel sensor and 20 mm Nikon lens. The Yoyo frame system also included a 200 watt-second Ocean Imaging Systems 3831 Strobe, an Ocean Imaging Systems model 494

bottom contact switch with weighted 1.5 m lanyard, and parallel red lasers for scaling. The camera was mounted on the frame looking vertically downward, prior to every deployment, with the underwater strobe offset by one meter, both were actuated with the bottom switch. The scaling lasers were checked before each deployment to make sure they were parallel and aimed directly downward 10 cm apart. The Yoyo Camera system was also equipped with a transmissometer providing real time data on shipboard, and an audible alarm, which sounded when the bottom contact switch closed, firing the camera. This allowed us to collect images of the seafloor at a high rate without dragging the camera or stirring up a large sediment cloud (resuspended sediment was detected by the transmissometer).



Figure 2.3: Yoyo Camera frame pre-deployment stage aboard the RV/IB-NBP. Shown in the image are the underwater camera (far right), strobe (far left), scaling lasers and bottom contact switch (center), and weighted 1.5 m lanyard (bottom center).

The survey method using the Yoyo Camera was the same across all stations and cruises with only minor variations of deployment. The only variation in our survey method was because of differences in deck the configurations of the RV/IB-NBP and the AS/RV-LMG. The larger RV/IB-NBP was configured with both an aft A-frame winch and starboard A-frame winch, while the smaller AS/RV-LMG was equipped with only an aft A-frame winch. Consequently, on both of our cruises aboard the AS/RV-LMG the camera frame was deployed from the aft A-frame winch, whereas during our austral winter cruise on the RV/IB-NBP the bottom camera was deployed midship from the starboard A-frame winch. Both methods worked well, however deployment from the starboard winch proved to be more suitable for collecting bottom pictures because of the reduced pitching motion midship.

Photo transects were completed at every station using the towed Yoyo Camera system. Each transect was assigned a unique deployment number (CRS #) (Table 2.1). Transects began at each station and proceeded in the best direction allowed by ice conditions and wind, which essentially randomized transect headings. Using an A-frame winch, the camera was lowered near to the seafloor and towed at a speed of ~1 knot. The camera was then lowered until the bottom-contact switch fired, then raised ~1.5 m off the seafloor and lowered again for the next firing. Each photo covered ~3 m<sup>2</sup> of seafloor. The time interval between photographs was about 15 s, yielding a spacing of 7 – 10 m between the centers of consecutive photos. Transects were terminated after transiting a 1 km linear distance or once 100 images of the seafloor had been collected, whichever came second. Replicate transects were completed at every station and on every cruise,

with the exception of station G on our third cruise during which time constraints and complications with the camera system allowed us to conduct only one transect of replicate transects with less than 100 usable images.

### **2.3. Data Processing**

Images collected during this study were color corrected, based on *in situ* images of a red-green-blue-white color chart, using Adobe ImageReady software. During our first cruise an Adobe ImageReady “droplet” (or mini-program) was created to correct the colors of the chart when photographed at depth during the first photo transects. Subsequent pictures taken on each cruise were color corrected using this droplet to adjust the proper color balance at depth (uncorrected images were heavily blue biased). This enabled us to exploit the high resolution of the camera and enhanced our abilities to distinguish animals, bioturbation features, and details in each image that would have been lost without color correction.

After color correction, bottom images were then imported as high-resolution jpegs into ImageJ software for scaling. Each individual picture was scaled in ImageJ using the 10 cm laser spots on the seafloor. Once an image was scaled it was saved as a TIF file so that the image scale, specific to each picture, was permanently attributed to that file as part of the image information (scaling is not saved in the jpeg file format). This allowed the file to be scaled only once and avoided the human error that would have been associated with having to rescale a jpeg file every time it was opened.

Following scaling in ImageJ, a 20 x 20 cm grid was overlain over each photo to

add a representative scale for animals in each image and aid in the compilation of an animal identification photo atlas. When an organism was found, a screen grab was taken of the animal. Screen grabs were then taken of exemplary and identifiable species in every image for all stations and cruises. After the compilation of the photo atlas, animals were identified and named using literature and reference material from trawl samples taken at every station.

Once photo atlases were completed for each station and a global photo atlas was compiled, animal counts for each CRS # were conducted using ImageJ's cell counter. A 30 x 30 cm grid was overlain on each photo and a count area of 1.8 m<sup>2</sup> in the center of each image was analyzed. Of the 100 or more images collected on each replicate photo transect, we randomly selected 50 photos for counting using an Excel random number generator. Due to sediment clouds, the random photos were adjusted slightly so that all the images counted had a clear central count area. This was not able to be accomplished on all transects and three transects had less than 50 countable pictures; CRS #1207 Sta.F cruise FB2-3 only had 46 countable pictures, CRS# 1208 Sta. F cruise FB2-3 had 43 countable pictures, and CRS #1205 (the only photo transect completed at Sta. G on cruise FB2-3) yielded 23 countable images. In total, 1,412 bottom photos covering 2542 m<sup>2</sup> were analyzed in this study (Table 2.1).

Table 2.1: Table of Number of Images Analyzed for each CRS# and Station									
Station AA	Image Count	Station B	Image Count	Station E	Image Count	Station F	Image Count	Station G	Image Count
CRS 947	50	CRS 961	50	CRS 976 (A)	50	CRS 990	50	CRS 1016	50
CRS 951	50	CRS 964	50	CRS 976 (B)	50	CRS 1005	50	CRS 1020	50
CRS 1113	50	CRS 1130	50	CRS 1091	50	CRS 1069	50	CRS 1054	50
CRS 1126	50	CRS 1132	50	CRS 1103	50	CRS 1072	50	CRS 1058	50
CRS 1232	50	CRS 1255	50	CRS 1217	50	CRS 1207	46	CRS 1205	23
CRS 1240	50	CRS 1267	50	CRS 1219	50	CRS 1208	43	N/A	0
<b>Total:</b>	<b>300</b>	<b>Total:</b>	<b>300</b>	<b>Total:</b>	<b>300</b>	<b>Total:</b>	<b>289</b>	<b>Total:</b>	<b>223</b>

Table 2.1: Table of the total number of bottom images analyzed for each photo transect (CRS#) and station.

## **2.4. Statistical Analysis**

Differences in abundance and species richness between stations and cruises were compared using non-parametric Kruskal-Wallis and Mann-Whitney tests. These statistical analyses were carried out using Minitab Statistical software v.15. Biodiversity analyses and community comparisons were conducted using PRIMER 6 software. Analyses conducted with PRIMER 6 included species accumulation plots by station (Ugland curves), estimates of total species richness by station (Chao 1, Chao 2, Jackknife and Bootstrap estimators), community similarity across all lowerings based on MDS using 4<sup>th</sup> root transformations to include contributions from both common and rare species, and Bray-Curtis Similarity.

## CHAPTER 3: RESULTS

### 3.1. Abundance

#### 3.1.1. Mean Abundance per m<sup>2</sup>

A total of 17,469 individual benthic megafauna, and 111 nektonic individuals, were counted in 1412 images. Station F had the highest densities of benthic megafauna (individuals per square meter) with CRS# 1069 and CRS# 1072 having the most animals per square meter of all transects, 13.89 per m<sup>2</sup> and 14.10 per m<sup>2</sup> respectively (Table 3.1). CRS# 1103 (Sta. E) and CRS# 1205 (Sta. G) had the lowest in the lowest densities of benthic megafauna of all transects with 1.77 and 3.77 individuals per m<sup>2</sup> (Table 3.1).

STATION AA		STATION B		STATION E		STATION F		STATION G	
Transect	Ind. per m <sup>2</sup>	Transect	Ind. per m <sup>2</sup>	Transect	Ind. per m <sup>2</sup>	Transect	Ind. per m <sup>2</sup>	Transect	Ind. per m <sup>2</sup>
CRS 947	10.87	CRS 961	6.03	CRS 976 (A)	3.71	CRS 990	13.47	CRS 1016	4.28
CRS 951	9.72	CRS 964	5.91	CRS 976 (B)	3.73	CRS 1005	10.97	CRS 1020	3.74
CRS 1113	7.02	CRS 1130	4.47	CRS 1091	3.02	CRS 1069	13.89	CRS 1054	3.07
CRS 1126	7.60	CRS 1132	4.37	CRS 1103	1.77	CRS 1072	14.10	CRS 1058	3.10
CRS 1232	9.59	CRS 1255	6.07	CRS 1217	3.34	CRS 1207	9.09	CRS 1205	3.77
CRS 1240	11.10	CRS 1267	5.37	CRS 1219	2.69	CRS 1208	12.74	N/A	N/A

Table 3.1: Table of mean abundance per meter squared for each photo transect. Transect column indicates photo transect label while the Ind. per m<sup>2</sup> column indicates average number of individuals seen per transect in a one meter square area.

Mean abundance per m<sup>2</sup> of each transect with standard error was then plotted by station to evaluate variability between transects. Figure 3.1 gives a graphical representation of the values in Table 3.1. For the most part, the abundances per m<sup>2</sup> for each transect did not vary much by station. Station AA and Station F had the largest spread of mean abundance per m<sup>2</sup> by transect, with differences of 5 - 7 individuals per m<sup>2</sup> between maximum and minimum abundance values (Figure 3.1).

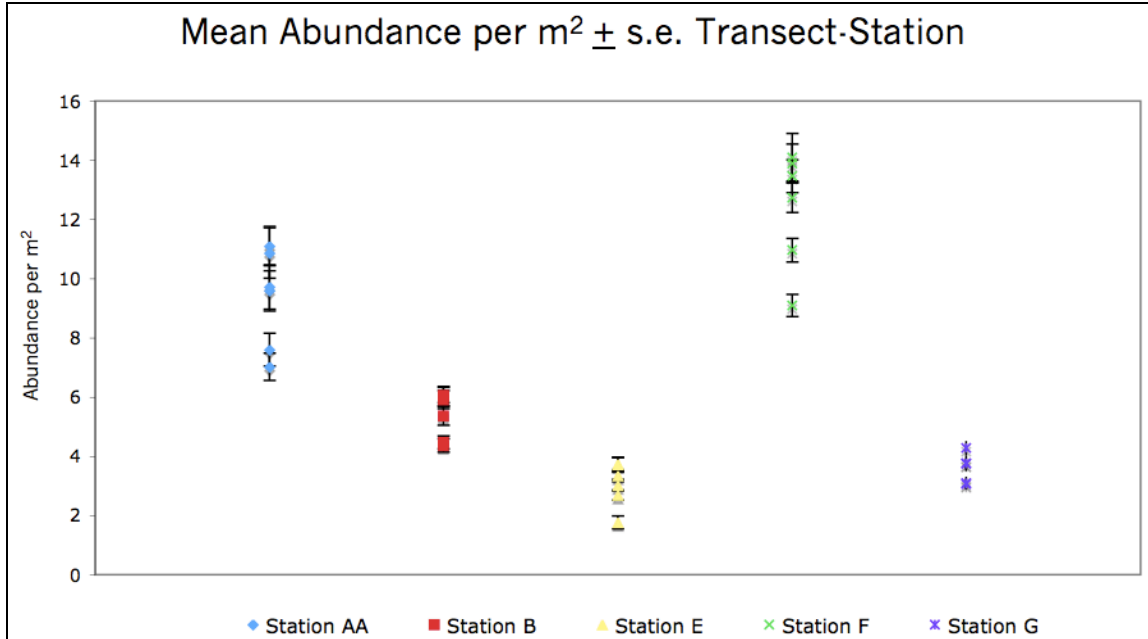


Figure 3.1: Plot of mean abundances per m<sup>2</sup> for each photo transect ± standard error. Each point indicates mean abundance per m<sup>2</sup> for an individual transect. Transects were then grouped by station to show mean abundance spreads between transects for each station.

### 3.1.2. Statistical Results for Abundance

Statistical tests were completed to determine whether or not there were significant differences in the mean megafaunal abundance per square meter between stations and also between cruises. The results of a Kruskal-Wallis Test for total abundances between stations showed that there were significant differences between stations ( $p = 0.000$ ,  $H = 871.97$ ,  $DF = 4$ ). A Kruskal-Wallis Test of abundances between cruises also indicated that there were significant differences between cruises ( $p = 0.000$ ,  $H = 922.01$ ,  $DF = 14$ ). Mann-Whitney tests were also carried out to determine whether or not there were significant differences between stations and between cruises.

The results of the Mann-Whitney Test between stations showed that there were significant differences between all stations (Table 3.2). Results from a Mann-Whitney Test of abundances between cruises showed that there were no significant differences between cruise FB-2-1 and FB-2-3 at Sta. AA ( $p = 0.4626$ ), FB-2-1 and FB-2-3 at Sta. B ( $p = 0.5938$ ), FB-2-3 Sta. AA and FB-2-3 Sta. F ( $p = 0.1381$ ), FB-2-2 Sta. B and FB-2-1 Sta. G ( $p = 0.0765$ ), FB-2-2 Sta. B and FB-2-3 Sta. G ( $p = 0.0575$ ), FB-2-1 Sta. E and FB-2-1 Sta. G ( $p = 0.2103$ ), FB-2-1 Sta. E and FB-2-1 Sta. G ( $p = 0.8525$ ), FB-2-3 Sta. E and FB-2-2 Sta. G ( $p = 0.8293$ ), and FB-2-1 Sta. G and FB-2-3 Sta. G ( $p = 0.4029$ ). A full table of p-values between cruises is located in the Appendix.

<b>Table 3.2: P-values for Mann-Whitney Test of total abundances between stations.</b>						
		<b>Mann-Whitney</b>				
		<b>Station AA</b>	<b>Station B</b>	<b>Station E</b>	<b>Station F</b>	<b>Station G</b>
<b>Mann-Whitney</b>			<<0.05	<<0.05	<<0.05	<<0.05
		<<0.05		<<0.05	<<0.05	<<0.05
		<<0.05	<<0.05		<<0.05	0.0002
		<<0.05	<<0.05	<<0.05		<<0.05
		<<0.05	<<0.05	0.0002	<<0.05	

### 3.1.3. Most Abundant Species

The ten most abundant species for each station were determined by their mean abundance per square meter from all transects. Table 3.3 shows the 10 dominant benthic megafauna at Sta. AA with Ophiuroid sp.2, Anemone sp.3, and *Notocrangon antarcticus* accounting for almost 90% of the total abundance at Sta. AA. The three most dominant species at Sta. B were *Chaetopterus* sp., Ophiuroid sp.4, and Pycnogonid sp.2, accounting for nearly 80% of the total abundance at Sta. B (Table 3.3). At Sta. E, *Chaetopterus* sp., Ampheliscid amphipod sp.1, and *Protelpidia murrayi*, accounted for approximately 75% of animals present (Table 3.3). *Chaetopterus* sp., *Rhipidothuria racowitzai*, and Ampheliscid amphipod sp.1 made up close to 90% of the total abundance of animals at Sta. F (Table 3.3). Sta. G's dominant three species made up the lowest percent of total abundance of all stations with *Chaetopterus* sp., *Protelpidia murrayi*, and Ophiuroid sp.4 being responsible for only ~58% of Sta. G's total abundance (Table 3.3). Of the ten dominant species at each station, *Notocrangon antarcticus* was the only species present at all stations while *Chaetopeterus* sp. was the most prevalent species at Sta. B, E, F, and G. Mysid sp.1 was also prevalent at Sta. AA, B, and E but was excluded from benthic megafaunal counts because it was always in the water column when photographed.

<b>Table 3.3: Top ten most abundant species for each station</b>		
<b>Station AA</b>	<b>% Tot. Abundance</b>	<b>Indiv. per m2</b>
Ophiuroid sp.2	80.1	7.48
Anemone sp.3	5	0.47
Notocrangon antarcticus	4.3	0.4
Anemone sp.1	2.5	0.23
Isopod sp.1	1.6	0.146
Pycnogonid sp.1	1.4	0.13
Anthomastus bathyproctus	1.3	0.117
Ophionotus victoriae	0.6	0.056
Flabellum impensum	0.5	0.048
Anemone sp.2	0.4	0.033
<b>Station B</b>	<b>% Tot. Abundance</b>	<b>Indiv. per m2</b>
Chaetopterus sp.	72	3.89
Ophiuroid sp.4	3.3	0.178
Pycnogonid sp.2	3	0.161
Notocrangon antarcticus	2.9	0.156
Ascidian sp.3	2.5	0.133
Pycnogonid sp.1	2.4	0.126
Anemone sp.1	2.1	0.115
Ascidian sp.2	1.8	0.098
Isopod sp.1	1.3	0.07
Peniagone vignioni	1.2	0.063
<b>Station E</b>	<b>% Tot. Abundance</b>	<b>Indiv. per m2</b>
Chaetopterus sp.	56.4	1.72
Ampheliscid amphipod sp.1	12	0.365
Protelpidia murrayi	6.3	0.193
Notocrangon antarcticus	6	0.17
Juvenile Elaspod sp.1	4.5	0.137
Ascidian sp.3	1.3	0.041
Bolocera kerguelensis	1.2	0.037
Pycnogonid sp.1	1.1	0.033
Scaleworm sp.1	1	0.031
Ophiuroid sp.4	1	0.031
<b>Station F</b>	<b>% Tot. Abundance</b>	<b>Indiv. per m2</b>
Chaetopterus sp.	75	41.7
Rhipidothuria racowitzai	8.7	4.83
Ampheliscid amphipod sp.1	4.9	2.72
Protelpidia murrayi	4.5	2.5
Notocrangon antarcticus	1.9	1.06
Isopod sp.2	1	0.556
Peniagone vignioni	0.7	0.389
Pycnogonid sp.2	0.6	0.333
Isopod sp.1	0.6	0.333
Ophiuroid sp.5	0.5	0.028
<b>Station G</b>	<b>% Tot. Abundance</b>	<b>Indiv. per m2</b>
Chaetopterus sp.	32.3	1.15
Protelpidia murrayi	19.7	0.705
Ophiuroid sp.4	6.4	0.229
Juvenile Elaspod sp.1	5.9	0.212
Notocrangon antarcticus	5.3	0.189
Golf Sponge sp.1	4.7	0.169
Sponge sp.1	3.9	0.14
Peniagone vignioni	3.8	0.135
Ampheliscid amphipod sp.1	2.4	0.085
Bolocera kerguelensis	1.9	0.067

## **3.2. Species Diversity**

There are two main components to species diversity: species richness, i.e. number of species present, and evenness, i.e., how uniformly distributed individuals are among species.

### **3.2.1. Species Richness and Accumulation**

The number of species collected at a station is dependent on sample size, until the full species list has been sampled. Thus, as transects were added and sample size increased, the likelihood that more species would accumulate also increased. Therefore, we used a variety of techniques to (1) determine that species were still accumulating at each station, and (2) estimate total species richness for each station. To understand how species diversity accumulated at each station as transects were added, we used an Uglund curve (UGE) which provides the mean species accumulation per transect at each station, based on 999 random orderings on of the transects (Figures 3.2 – 3.6).

As seen in Figure 3.2 to Figure 3.6 the UGE curve is still increasing at all stations after all transects have been added. This indicates that species are still accumulating at every station and we did not sample all of the species present at any station. Therefore, we used multiple species richness estimators to compare species richness between stations. The estimators we used to estimate total species richness at each station were the Chao 1, Chao 2, Jackknife, and Bootstrap estimators, Figures 3.2 – 3.6.

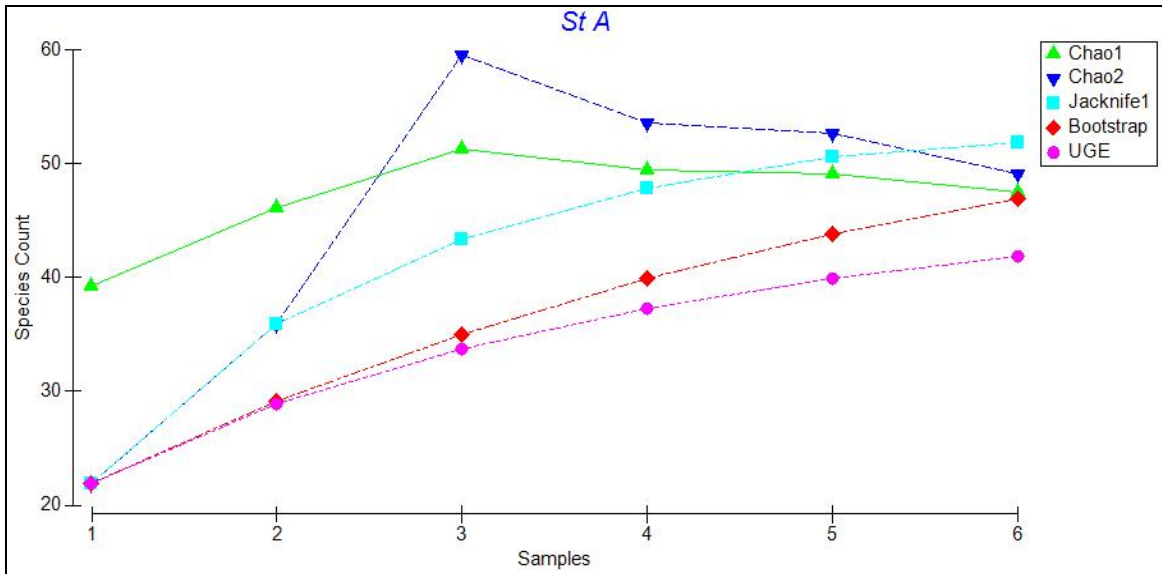


Figure 3.2: Plot of five species estimators for Station AA: Chao 1, Chao 2, Jackknife 1, Bootstrap, and Uglund. Species counts refer to total number of species and samples correspond to additional photo transects (i.e. sample 1 is the first transect, sample 2 is transect 1 plus transect 2, etc.).

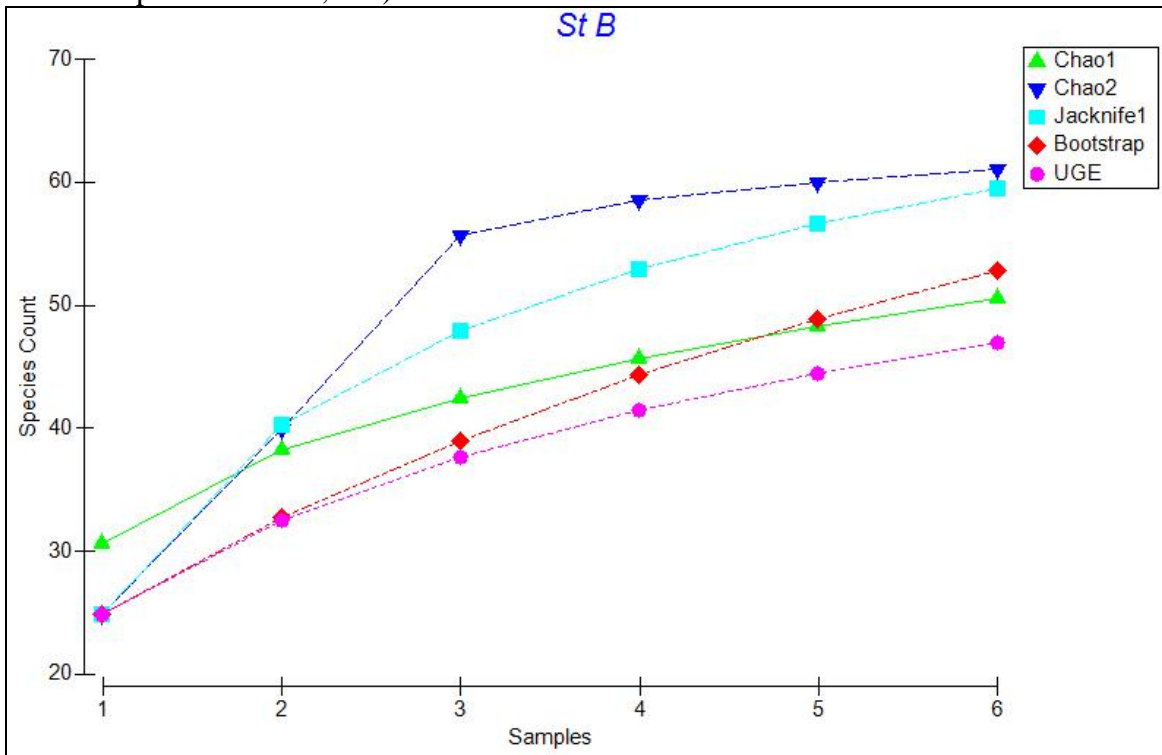


Figure 3.3: Plot of five species estimators for Station B: Chao 1, Chao 2, Jackknife 1, Bootstrap, and Uglund. Species counts refer to total number of species and samples correspond to additional photo transects (i.e. sample 1 is the first transect, sample 2 is transect 1 plus transect 2, etc.).

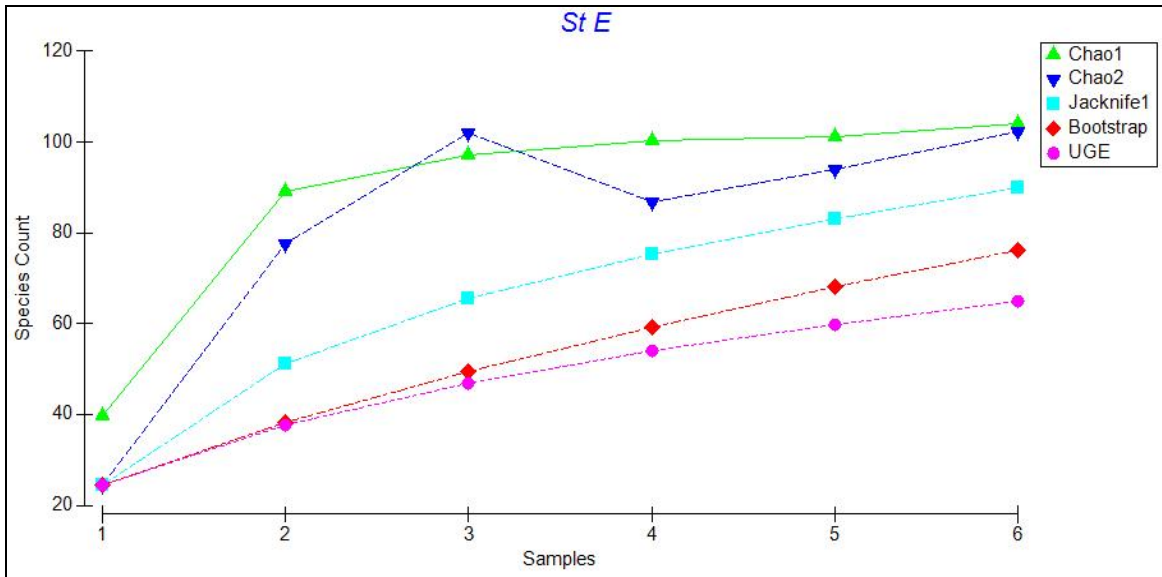


Figure 3.4: Plot of five species estimators for Station E: Chao 1, Chao 2, Jackknife 1, Bootstrap, and Uglund. Species counts refer to total number of species and samples correspond to additional photo transects (i.e. sample 1 is the first transect, sample 2 is transect 1 plus transect 2, etc.).

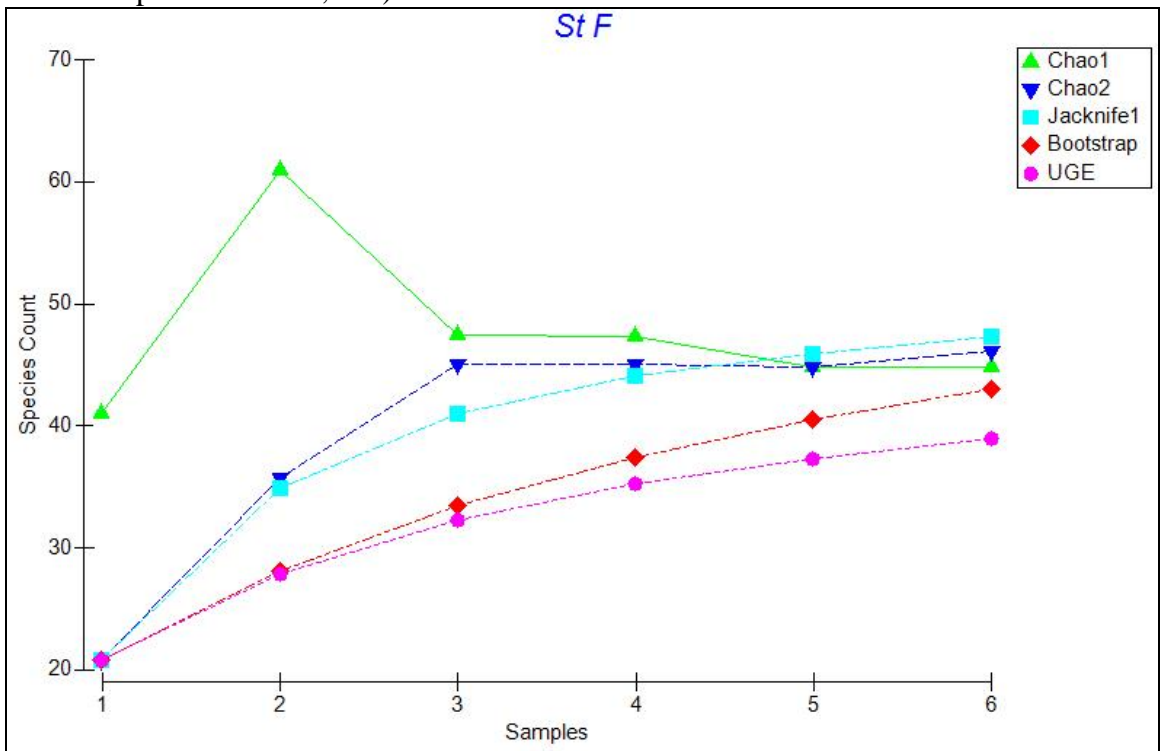


Figure 3.5: Plot of five species estimators for Station F: Chao 1, Chao 2, Jackknife 1, Bootstrap, and Uglund. Species counts refer to total number of species and samples correspond to additional photo transects (i.e. sample 1 is the first transect, sample 2 is transect 1 plus transect 2, etc.).

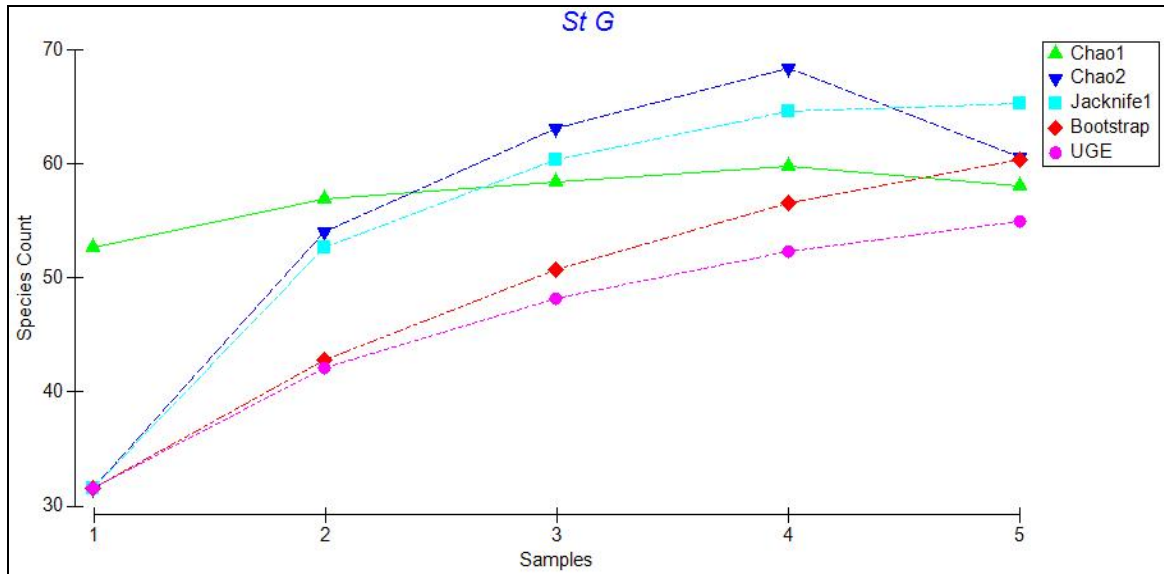


Figure 3.6: Plot of five species estimators for Station G: Chao 1, Chao 2, Jackknife 1, Bootstrap, and Uglan. Species counts refer to total number of species and samples correspond to additional photo transects (i.e. sample 1 is the first transect, sample 2 is transect 1 plus transect 2, etc.).

Figures 3.2 to 3.6 indicate that these estimators generally agree at all stations, therefore we used Chao 1 for our comparisons. A plot of Chao 1 with  $\pm$  one standard error shows that species richness is similar across all stations except Sta. E (Figure 3.7). Station E has many species that occur as singletons (only one individual of that species observed), giving a much higher and more variable value for the Chao 1 species richness estimator. Other species richness estimators also show a peak in species richness at Sta. E, although this peak is less marked, especially for the Bootstrap estimator. Nonetheless, for all the species richness estimators, there is no obvious latitudinal trend in estimated species richness along the sampling transect.

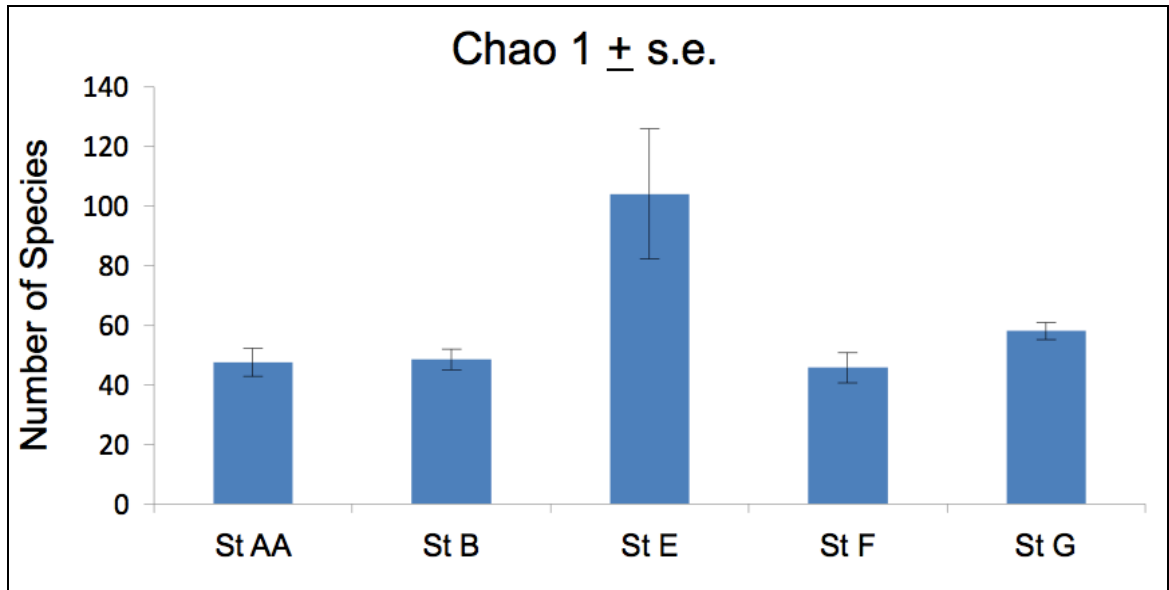


Figure 3.7: Plot of Chao 1 estimator values for all stations  $\pm$  standard error. The number of species corresponds to the total number of species that could be expected at each station with infinite sampling effort.

### 3.2.2. Evenness and Rarefaction

The second component of species diversity, evenness, can be assessed with two metrics: (a) Rarefaction diversity, which evaluates both richness and evenness, and (b)  $J'$ , a strict species evenness index. Once again, evenness refers to how uniformly distributed individuals are between species. The Rarefaction diversity for each station with the expected number of species in a sub sample of 150 individuals,  $Es(150)$ , is plotted in Figure 3.8, and Evenness  $J'$  for each station is shown in Figure 3.9. Both indices show a nearly latitudinal trend, however, Sta. F and Sta. AA have similarly low diversity indexes. Mann-Whitney Tests were used to test for significant differences in the means of  $Es(150)$  and Evenness  $J'$  values. There were no significant differences for the mean values for the  $Es(150)$  index between Sta. AA and Sta. F ( $p = 0.4712$ ), and Sta. B and Sta. E ( $p =$

0.2298). The Mann-Whitney Test of the Evenness J' index indicated that there was no significant difference between Sta. AA and Sta. F ( $p = 0.0927$ ). Mann-Whitney p-value tables for Es(150) and Evenness J' indices are located in Appendix.

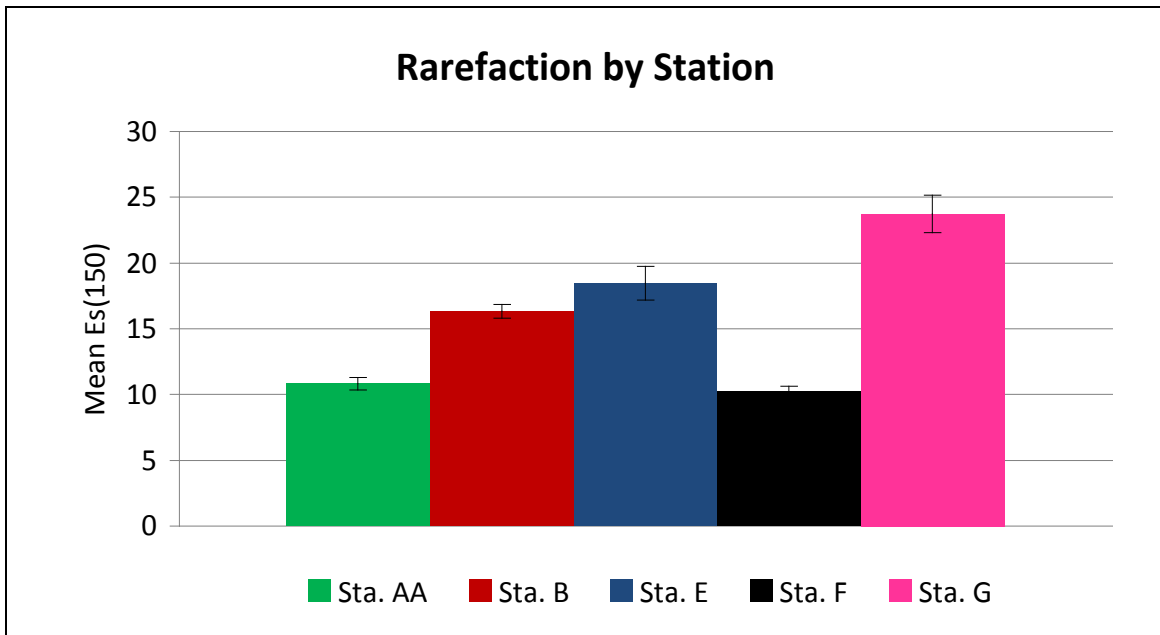


Figure 3.8: Plot of Rarefaction for each station. Mean Es(150) values correspond to the total number of species that would be expected in a sub sample size of 150 images for each station.

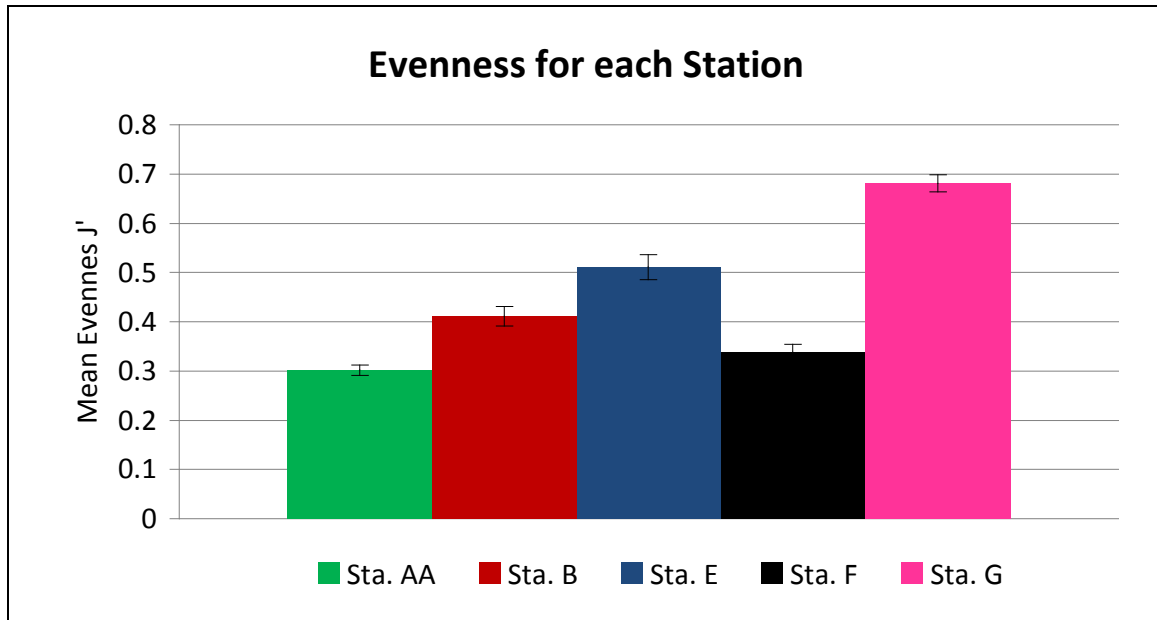


Figure 3.9: Plot of Evenness for each station. Evenness  $J'$  values correspond to a uniform distribution indicator value. Higher values indicate increased uniform distribution of individuals between species present at each station and lower indicate decreased uniform distribution (i.e. less biodiversity).

### 3.3. Community Composition

#### 3.3.1. Community Structure

Community structure was compared between transects and stations using a non-Metric Multidimensional Scaling analysis. The results from this analysis are plotted in Figure 3.10. The results indicate that there three basic clusters: Sta. AA, Sta. B, and a combined cluster of Sta. E, F, and G. This suggests Sta. AA is distinct from all other stations in both species identifications and proportions. The separation distance of cluster Sta. B, in Figure 3.10, indicates that Sta. B is very different from Sta. AA and only somewhat different from the Sta. E, F, and G cluster. The MDS 4<sup>th</sup> root plot, Figure 3.10, also suggests that there is a gradual shift in community structure along the sampling transect from Sta. AA to Sta. G.

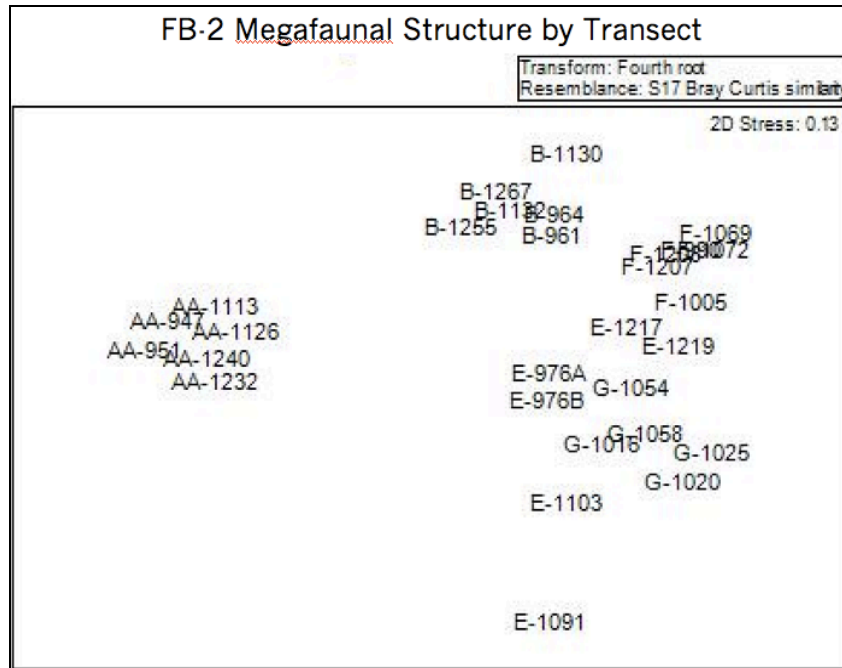


Figure 3.10: Non-metric Multidimensional Scaling plot of species community structure similarity between all transects. Three main clusters: Sta. AA, Sta. B, and Stas. E,F, and G. Transect scaling is based on presence-absence data from Bray-Curtis index for each transect.

The non-Metric Multidimensional Scaling (nMDS) analyses used a Bray-Curtis similarity index of presence-absence data to compare community structure across transects. As seen in Figure 3.11, the abrupt changes in community structure between Sta. AA, B, and E result from this similarity index and are due to the differences in proportions and identities of species across stations. The Bray-Curtis Similarity plot, Figure 3.11, shows that stations share 30-40% of their species across the entire station transect (Sta. AA-G).

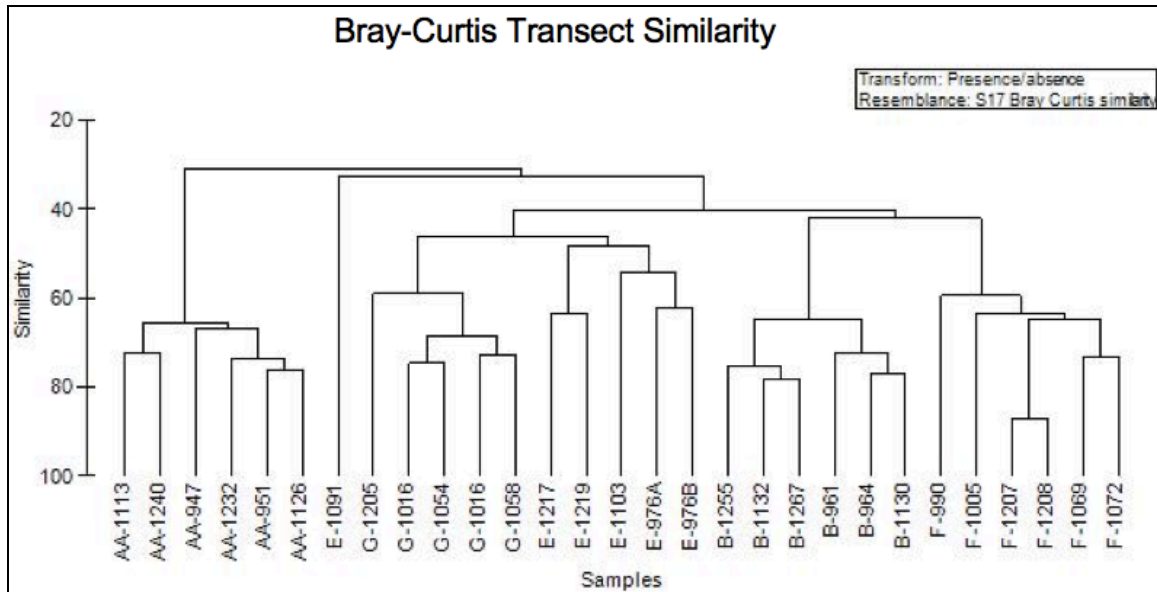


Figure 3.11: Bray-Curtis plot of similarity between all photo transects. Similarity index is based on presence-absence data for species at each station. Similarity values indicate the percentage of species that are shared by each transect. Samples correspond to species lists for individual transects (i.e. AA-1113 = Station AA CRS# 1113, etc.).

### 3.3.2. Functional Groups

Functional groups analyses were conducted by assigning all species counted in this study, except for nekton, one of seven functional group labels based on locomotion type and feeding characteristics. Functional groups were as follows: m/so (mobile, suspension feeder), s/so (sessile, scavenger/omnivore), m/sf (mobile, suspension feeder), s/sf (sessile, suspension feeder), m/df (mobile, deposit feeder), s/df (sessile, suspension feeder), and m/c (mobile, carnivore). Functional group structure for each station was then analyzed by examining the percent of the total individuals per station that each functional group represented, as shown in Figure 3.12.

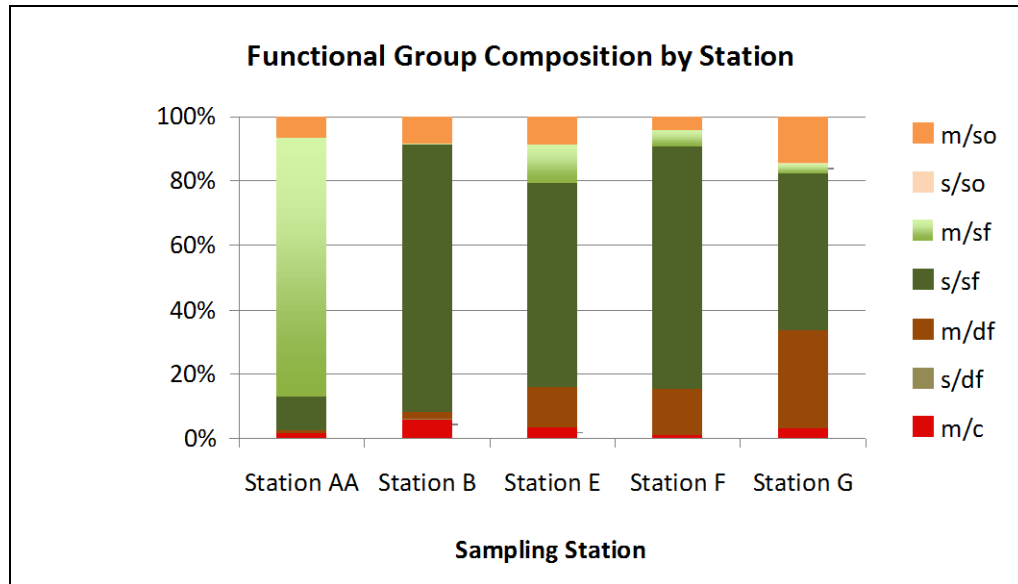


Figure 3.12: Plot of functional group composition for each station. Percent of total abundance corresponds to the percent of individuals for each functional group that make up the total abundance at each station. Functional groups are: m/c (mobile carnivore), s/df (sessile suspension feeder), m/df (mobile deposit feeder), s/sf (sessile suspension feeder), m/sf (mobile suspension feeder), s/so (sessile scavenger/omnivore), and m/so (mobile scavenger/omnivore).

Functional group structure varied dramatically along the sampling transect.

Station AA was dominated by mobile suspension feeders, while the remaining stations were dominated by sessile suspension feeders (mostly *Chaetopterus* sp.). The percentage of mobile deposit feeders increased dramatically from north to south along our sampling transect. *Chaetopterus* sp. was the lone infaunal species reliably counted due to its characteristic burrow; if we restrict our functional group analysis to the epibenthic megafauna, which we well censused, the increase in mobile deposit feeders with latitude is even more dramatic, rising monotonically from near zero at Sta. AA to ~ 50% at Station G. Within the epibenthic megafauna, total suspension feeders also decline dramatically with latitude, from ~80% at Sta. AA to ~8-15% at Stas. F and G.

## CHAPTER 4: DISCUSSION

Sea ice is an important driver in determining marine ecosystem structure along the WAP. As mentioned earlier, primary production in the upper surface waters of the WAP is directly affected by the extent and duration of seasonal sea ice and therefore, sea ice plays a central role in determining food supply and ecosystem structure on the WAP continental shelf. The initial hypotheses presented in this study; that megafaunal abundance, biodiversity, and community structure would vary latitudinally due to seasonal sea ice, were based on these assumptions. The results from our survey of the benthos of WAP continental shelf indicate that, while sea ice is a primary driver of ecosystem structure, it is definitely not the only driving force of a much more complicated system. These findings will be discussed in detail based on our three main criteria for benthic megafaunal ecosystem structure: abundance, species richness, and community composition.

### **4.1. Abundance**

The first hypothesis posed in this study was that benthic megafaunal abundance of the WAP continental shelf would vary latitudinally along our strong sea ice gradient transect. Our findings are consistent with this hypothesis to some extent but did not show a pronounced monotonic trend along our sampling transect. Benthic megafaunal abundance was assessed for each of our sampling stations along the WAP based on

abundance of megafaunal individuals per m<sup>2</sup> for each transect and also by the 10 most dominant species at each station.

Abundance per m<sup>2</sup> varied for each transect and ranges of mean abundances varied by station with most stations showing a small amount of variance between transects (Figure 3.1 and Table 3.1). Interestingly, our two stations that showed the most variance between mean abundance per m<sup>2</sup> for each transect, AA and F, also corresponded to the highest mean abundance per m<sup>2</sup> values seen. This higher degree of variance may be due to higher levels of productivity allowing a broader range of food-rich and food-poor patches on the seafloor. However, this would not seem to be the case at station F due to the thought that the increased sea ice duration associated with F would limit primary production. Therefore, productivity level, as consequence of sea ice duration, does not seem to be the sole primary driver of benthic megafaunal mean abundances at station F. A potential cause for the higher variance of mean abundances at F may in fact indicate that at station F we sampled more habitat niches in which a few specific benthic species are able to thrive in high abundances.

In general, our data illustrates a trend of decreasing mean abundance from north to south along the WAP corresponding to increasing sea ice duration along our transect. This decreasing trend is what we had expected to see due to the assumption that increased sea ice implies shorter phytoplankton blooms and reduced food availability to the water column and benthos. However, Station F (Figure 3.1) did not necessarily follow the general decreasing trend and showed a large increase in mean abundance values. As noted above, it is difficult to know the exact causes for the large increase at station F

without examining which species characterize the majority of mean abundance per square meter.

Therefore, in order to understand how megafaunal abundance varies along our sampling transect with respect to sea ice, it is also important to know what species compose our abundance per  $m^2$  values. By breaking down total abundance and per  $m^2$  values for the 10 most dominant species at each station we were able to more clearly comprehend the trends seen between photo transects for each station. All stations were characterized by a few species dominating the majority of total abundance and per  $m^2$  values. Interestingly, the species lists for the top 10 species at each station varied dramatically from station to station with only one species, *Notocrangon antarcticus*, being in the top ten of all stations. A second species, *Chaetopterus* sp., was the dominant species at stations B, E, F, and G making up ~72, 56, 75, and 32 % of total abundance for each station respectively. These values are somewhat misleading and infer that *Chaetopterus* sp. was seen in similar abundances at stations B, E, F, and G. However, taking a closer looking at per  $m^2$  values for each station it is apparent that stations B, E, and G have much lower abundances of *Chaetopterus* sp. (ranging from ~1-4 individuals per  $m^2$ ) than station F where abundances of *Chaetopterus* sp. are particularly high (~42 individuals per  $m^2$ ), as seen in Table 3.3. Therefore, the large increase in megafaunal abundance per  $m^2$  seen at station F, Figure 3.1, is solely due to a single species.

However, *Chaetopterus* sp. is considered an infaunal species (one of two infaunal species counted), as opposed to epibenthic megafauna, and therefore when included in this study it may give a biased representation of megafaunal abundances because other

abundant infaunal species could not be counted. If we exclude *Chaetopterus* sp. and focus on epibenthic megafauna, which were efficiently counted at all stations, our abundance per m<sup>2</sup> values indicate a distinct decreasing trend from north to south of megafaunal mean abundance per m<sup>2</sup>. Also, the mean abundance per square meter values for photo transects at F show a much lower variance (Appendix) and therefore refutes the possibility that the higher variance seen in Figure 3.1 for station F could be a result of sampling more habitat niches. It is also important to note that when *Chaetopterus* sp. other infaunal species are removed, the dominant majority species for each station changes: Ophiuroid sp. 4 – Sta. B, *Protelpida murrayi* – Sta. E, *Rhipidothuria racowitzai* – Sta. F, and *Protelpida murrayi* – Sta. G. (Appendix). Also, for the epibenthic megafauna, stations B, E, F, and G show more even relative abundance across the most dominant 10 species (Appendix). Consequently, in support of our initial hypothesis, epibenthic megafaunal abundance does in fact vary along our strong sea ice gradient transect from north to south with an overall decreasing trend in the abundance of individuals per m<sup>2</sup> from north to south as a result of sea ice duration.

#### **4.2. Species Richness**

The next goal of this study was to determine whether species richness varies along our sampling transect concomitantly with sea ice duration, as hypothesized.

We used UGE species accumulation curves, potential species richness estimators, and two biodiversity indices (Rarefaction and Evenness) to investigate species richness and evenness aspects of species diversity.

Estimating species accumulation for each station was based on two key questions. The first question we needed to answer was whether our sampling effort was adequate enough to have completely sampled the species list at each station. By using UGE species accumulation curves, we were able to distinguish whether our stations were still accumulating species with additional photo transects. Figures 3.2 – 3.6 show plots of the UGE curve (purple) for each station. We see that each of our stations is still accumulating species due to the fact that the UGE curve has yet to reach an asymptote at any station (Figures 3.2 - 3.6). However, while the slope of the UGE is still increasing at all stations, the shallow slope indicates that as more samples are added we do not expect to accumulate new species at a very high rate. The fact that all stations are still accumulating species is pretty remarkable considering 1,300 to >5,000 megafaunal individuals were identified at each station.

The next step to understanding species accumulation was accomplished by estimating how many species could be expected at each station with infinite sampling efforts. We used a range of species accumulation estimators (Chao 1, Chao 2, Bootstrap, and Jackknife 1) to estimate total species richness for each station. As seen in Figures 3.2 – 3.6, all species estimator curves for each station follow show a general increasing trend. Therefore, since all curves showed similar trends we chose to use the Chao 1 curve to indicate estimated species accumulation or richness at each station. Our Chao 1 estimates of total species richness show no real trend or pattern across our sampling stations with most estimated values at Stations AA, B, F and G being within 3 - 5 species of the number of found at each station. However, Chao 1 suggested that station E had many

more species to be sampled, with about 40 more species expected at station E with infinite sampling.

The expected ~104 species at station E indicated by our Chao 1 index is almost as high as our total species list for all stations of 109 benthic megafauna. We believe that this estimate is an over estimate of total species richness for station E and is due to the fact that Chao 1 is based solely on the number of singleton and doubleton species seen at each station (the number of species found only once and twice in a photo transect). While it is true that station E had a much higher number of rare species (species seen once or twice) compared to all other stations, it is possible that the increase in singletons and doubletons is due to potentially greater habitat heterogeneity owed to the presence of increased rocky substrate at E. Even though megafaunal individuals located on rocks were not counted, the mix of complex rocky habitat and soft sediment could contribute to the high Chao 1 value seen at station E (other estimators show high values for E but not nearly as high). Consequently, species richness and accumulation estimators showed no general trend along our sampling transect.

Biodiversity was determined for each station using two different species richness indicators, Rarefaction and Evenness,  $J'$ . Rarefaction was used to evaluate biodiversity at each of our stations by determining how many species could be expected to be seen in a sub sample of 150 individuals at each station. Conversely, Evenness  $J'$  is an index strictly of evenness, or uniformity of distribution of species among individuals counted. Both indicators showed similar patterns (Figures 3.8 and 3.9). Station G showed the highest

degree of evenness. Overall, stations show increasing evenness ( $J'$ ) and total biodiversity (Rarefaction) along our sampling transect from AA to G with a distinct drop at station F, as seen in Figures 3.8 and 3.9.

The large decrease in both Evenness $J'$  and Rarefaction associated with F is due primarily to two species dominating station F's megafaunal abundance. *Chaetopterus* sp. (polychaete) and *Rhipidothuria racowitzai* (elaspod holothurian) account for ~ 75% (~42 indiv. per m<sup>2</sup>) and 9% (~5 indiv. per m<sup>2</sup>) respectively of total abundance at station F (Table 3.3). As mentioned earlier, *Chaetopterus* sp. is considered an infaunal species and when included it gives an inaccurate representation of megafaunal abundance. Consequently, we believe that if *Chaetopterus* sp. is ignored in both Rarefaction and Evenness $J'$  then both values for station F will increase and a much more distinct trend of increased biodiversity and evenness could be seen from north to south along our transect. However, due to the large drop associated with station F our data indicates no real latitudinal trend regarding benthic megafaunal species richness and biodiversity from station AA to station G. Still, our data indicates that more species are able to survive further south, possibly because it is difficult for single epibenthic megafaunal species to dominate in such low food environments, allowing more species to establish themselves. Future publications will reassess all indicators without *Chaetopterus* sp.. Therefore, with respect to all four species richness measures, we saw no latitudinal trend along our transect with the key findings being that while all stations are still accumulating species, most are relatively well sampled.

### 4.3. Community Composition

Lastly, benthic megafaunal community structure and trophic complexity were analyzed for all of our stations to test our third and final hypothesis. Our final hypothesis predicts that benthic megafaunal community composition will vary along a strong sea ice gradient on the WAP continental shelf. This hypothesis was evaluated by comparing community structure across transects using Bray-Curtis Similarity and Non-Metric Multidimensional Scaling and by examining functional group composition for each station.

The process of analyzing community structure along our sampling transect was achieved by creating both a Bray-Curtis similarity dendrogram consisting of all individual photo transects (Figure 3.11) and a Non-Metric Multidimensional Scaling plot (nMDS) (Figure 3.10). Looking at our Bray-Curtis dendrogram (Figure 3.11), it is apparent that transects within stations show the greatest degree of similarity in megafaunal community structure and that certain stations are similar in structure. It is also important to note that 30 – 40% of all species are shared across all stations. This indicates that certain benthic megafaunal species are well established and widely distributed along the WAP continental shelf.

Our nMDS plot (Figure 3.10) illustrates that when all transects are compared, three distinct clusters of similar community structure appear. We see a gradual change of megafaunal community structure along our transect from station AA to station G. The scale of separation between clusters and the degree of variance between clustered

transects demonstrates this change. Our first cluster, made up exclusively of station AA transects, demonstrates the lowest variance of all clusters and based on separation is the most different in community structure from all other transects and clusters (Figure 3.10). Moving along our transect, the second cluster seen in our nMDS plot consists of only station B transects and is very distinct from our first cluster but is only somewhat different in community structure from our third cluster, which is comprised of transects from stations E, F, and G with the highest variance. Consequently, we are able to show that community structure varies gradually along our sampling transect.

However, when examining overall community composition for each of our stations along the WAP with respect to sea ice duration, it is also important to evaluate trends in benthic megafaunal trophic complexity. Trophic complexity was assessed based on functional group data for each station and plotted in Figure 3.12. As seen in Figure 3.12, functional group structure varied dramatically by station, however, two clear trends are evident. The first trend illustrated shows a continuous decrease in both mobile and sessile suspension feeders along our transect. For example, suspension feeders characterize ~90 % of total abundance at station AA, ~70 % of total abundance at station B, and decline to about ~50 % of total abundance at our most southern station G. Conversely, mobile deposit feeders show an opposite trend while increasing from about ~1 % of total abundance at AA to making up ~30 % of total abundance at station G. These trends both are consistent with the ‘foodbank’ hypothesis that, due to longer sea ice seasons further south, shorter summer phytoplankton blooms will cause greater ecological selection for benthic megafaunal feeding types that can use phytodetritus

accumulated on the seafloor throughout the winter (Smith et al. 2006). Therefore, our benthic megafaunal community structure and trophic complexity data strongly support our final hypothesis that megafaunal community composition would vary long the WAP in concert with sea ice duration.

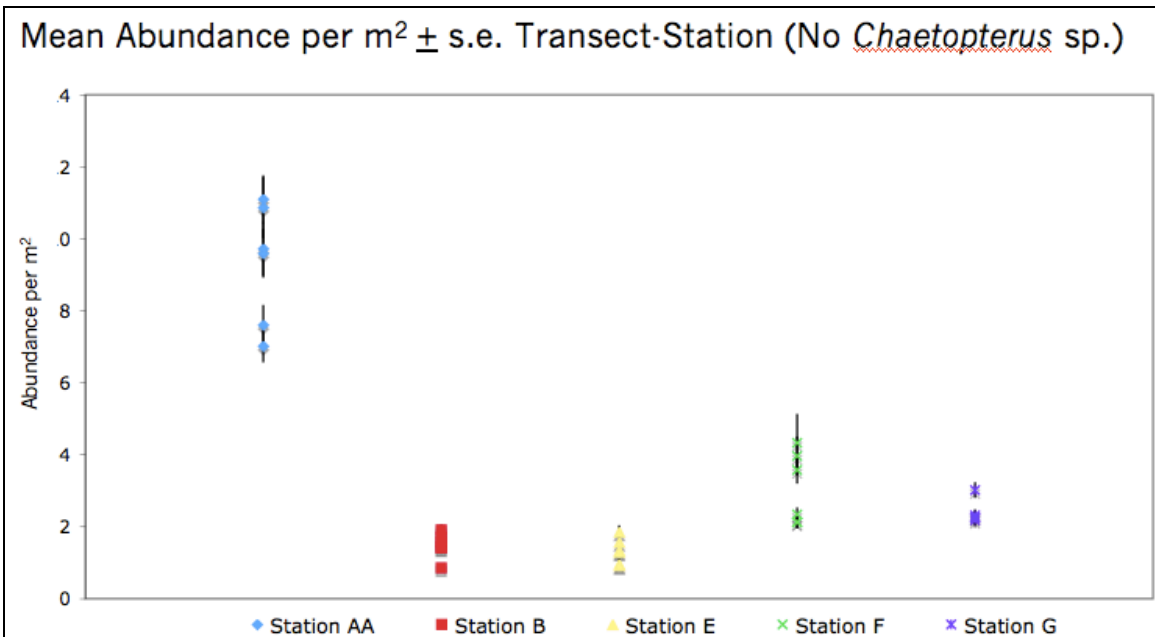
#### **4.4. Conclusion**

In summary, we conclude that benthic megafaunal abundance and community composition will change along the WAP due to sea ice loss as a consequence of regional climate change. However, due to potential biases in our data for species richness, we can not conclude that benthic megafaunal species richness will vary with any general trend as a result of decreased sea ice duration along the WAP. In the end, this research is important because rapid climate change is reducing annual sea ice duration on the WAP and fundamentally affecting primary production and pelagic community structure. This is expected to influence the flux of food material and food type to the benthos living on the Antarctic continental shelf. By evaluating how benthic community structure, abundance, and biodiversity vary with latitudinal differences in sea extent and duration, we should be able to predict how Antarctic marine ecosystems will change along the WAP as a consequence of sea ice loss due to climate change.

# APPENDIX

Table of p-values for Mann-Whitney Test of total abundances between cruises and stations.																	
	Station AA			Station B			Station E			Station F			Station G				
	FB-2-1	FB-2-2	FB-2-3	FB-2-1	FB-2-2	FB-2-3	FB-2-1	FB-2-2	FB-2-3	FB-2-1	FB-2-2	FB-2-3	FB-2-1	FB-2-2	FB-2-3		
Station AA	FB-2-1		0.0001	0.4624	<<0.05	<<0.05	<<0.05	<<0.05	<<0.05	<<0.05	<<0.05	0.0001	<<0.05	0.0379	<<0.05	<<0.05	<<0.05
	FB-2-2	0.0001		<<0.05	0.0177	<<0.05	0.0044	<<0.05	<<0.05	<<0.05	<<0.05	<<0.05	<<0.05	<<0.05	<<0.05	<<0.05	<<0.05
	FB-2-3	0.4624	<<0.05		<<0.05	<<0.05	<<0.05	<<0.05	<<0.05	0.0002	<<0.05	0.1381	<<0.05	<<0.05	<<0.05	<<0.05	<<0.05
Station B	FB-2-1	<<0.05	0.0177	<<0.05		<<0.05	0.5938	<<0.05	<<0.05	<<0.05	<<0.05	<<0.05	<<0.05	<<0.05	<<0.05	<<0.05	<<0.05
	FB-2-2	<<0.05	<<0.05	<<0.05	<<0.05		<<0.05	0.0041	<<0.05	<<0.05	<<0.05	<<0.05	<<0.05	0.0765	<<0.05	0.0575	
	FB-2-3	<<0.05	0.0044	<<0.05	0.5938	<<0.05		<<0.05	<<0.05	<<0.05	<<0.05	<<0.05	<<0.05	<<0.05	<<0.05	<<0.05	<<0.05
Station E	FB-2-1	<<0.05	<<0.05	<<0.05	<<0.05	0.0041	<<0.05		<<0.05	0.0031	<<0.05	<<0.05	<<0.05	0.2103	0.0063	0.8525	
	FB-2-2	<<0.05	<<0.05	<<0.05	<<0.05	<<0.05	<<0.05			0.0016	<<0.05	<<0.05	<<0.05	<<0.05	0.0007	0.0002	
	FB-2-3	<<0.05	<<0.05	<<0.05	<<0.05	<<0.05	0.0031	0.0016			<<0.05	<<0.05	<<0.05	<<0.05	0.8293	0.0191	
Station F	FB-2-1	0.0001	<<0.05	0.0002	<<0.05	<<0.05	<<0.05	<<0.05	<<0.05		0.0168	0.0094	<<0.05	<<0.05	<<0.05	<<0.05	
	FB-2-2	<<0.05	<<0.05	<<0.05	<<0.05	<<0.05	<<0.05	<<0.05	<<0.05	0.0168		<<0.05	<<0.05	<<0.05	<<0.05	<<0.05	
	FB-2-3	0.0379	<<0.05	0.1381	<<0.05	<<0.05	<<0.05	<<0.05	<<0.05	0.0094	<<0.05		<<0.05	<<0.05	<<0.05	<<0.05	
Station G	FB-2-1	<<0.05	<<0.05	<<0.05	<<0.05	0.0765	<<0.05	0.2103	<<0.05	<<0.05	<<0.05	<<0.05			<<0.05	0.4029	
	FB-2-2	<<0.05	<<0.05	<<0.05	<<0.05	<<0.05	<<0.05	0.0063	0.0007	0.8293	<<0.05	<<0.05	<<0.05	<<0.05		0.0214	
	FB-2-3	<<0.05	<<0.05	<<0.05	<<0.05	0.0575	<<0.05	0.8525	0.0002	0.0191	<<0.05	<<0.05	<<0.05	0.4029	0.0214		

Table of p-values for Mann-Whitney Test of total abundances between cruises and stations. Sub columns and rows indicate separate cruises for each main column and row indicating station. Grey coloring is used to break up the table while yellow indicates significant p-values.



<b>Table 3.3: Top ten most abundant species for each station</b>		
<b>Station AA</b>	<b>% Tot. Abundance</b>	<b>Indiv. per m2</b>
Ophiuroid sp.2	80.3	7.48
Anemone sp.3	5	0.47
Notocrangon antarcticus	4.3	0.4
Anemone sp.1	2.5	0.23
Isopod sp.1	1.6	0.146
Pycnogonid sp.1	1.4	0.13
Anthomastus bathyproctus	1.3	0.117
Ophionotus victoriae	0.6	0.056
Flabellum impensum	0.5	0.048
Anemone sp.2	0.4	0.033
<b>Station B</b>	<b>% Tot. Abundance</b>	<b>Indiv. per m2</b>
Ophiuroid sp.4	12	0.178
Pycnogonid sp.2	10.9	0.161
Notocrangon antarcticus	10.5	0.156
Ascidian sp.3	9	0.133
Pycnogonid sp.1	8.5	0.126
Anemone sp.1	7.8	0.115
Ascidian sp.2	6.6	0.098
Isopod sp.1	4.8	0.07
Peniagone vignioni	4.3	0.063
Anemone sp.4	3.8	0.056
<b>Station E</b>	<b>% Tot. Abundance</b>	<b>Indiv. per m2</b>
Protelpidia murrayi	20	0.193
Notocrangon antarcticus	17.7	0.17
Juvenile Elasipod sp.1	14.3	0.137
Ascidian sp.3	4.2	0.041
Bolocera kerguelensis	3.9	0.037
Pycnogonid sp.1	3.5	0.033
Scaleworm sp.1	3.3	0.031
Ophiuroid sp.4	2.9	0.028
Ophiuroid sp.5	2.5	0.024
Sterechinus antarcticus	2.5	0.024
<b>Station F</b>	<b>% Tot. Abundance</b>	<b>Indiv. per m2</b>
Rhipidothuria racowitzai	43	1.077
Protelpidia murrayi	22.2	0.556
Notocrangon antarcticus	9.1	0.227
Isopod sp.2	5.1	0.127
Peniagone vignioni	3.6	0.088
Pycnogonid sp.2	3	0.075
Isopod sp.1	2.8	0.071
Ophiuroid sp.5	2.6	0.065
Flabelligera sp.	1.1	0.029
Irr. Urchin sp.3	1.1	0.029
<b>Station G</b>	<b>% Tot. Abundance</b>	<b>Indiv. per m2</b>
Protelpidia murrayi	30.2	0.705
Ophiuroid sp.4	9.8	0.229
Juvenile Elasipod sp.1	9.1	0.212
Notocrangon antarcticus	8.1	0.189
Golf Sponge sp.1	7.3	0.169
Sponge sp.1	6	0.14
Peniagone vignioni	5.8	0.135
Bolocera kerguelensis	2.9	0.067
Ophiuroid sp.5	2.6	0.06
Anemone sp.7, Cerianthid	1.3	0.03

## REFERENCES

- ARRIGO, K. R., G. L. VAN DIJKEN, S. BUSHINSKY (2008), Primary production in the Southern Ocean, 1997–2006, *J. Geophys. Res.*, 113, C08004, doi:10.1029/2007JC004551.
- BARNETT, T. P., PIERCE, D. W., ACHUTARAO, K. M., LECKER, P. J., SANTER, B. D., GREGORY, J. M. & WASHINGTON, W. M. (2005), Penetration of human-induced warming into the world's oceans. *Science* 309, 284–287.
- CLARKE, A., JOHNSTON, N.M., (2003), Antarctic marine benthic diversity. *Oceanography and Marine Biology: An Annual Review* 41, 47–114.
- CLARKE, A., MURPHY, E. J., MEREDITH, M. P., KING, J. C., PECK, L. S., BARNES, D. K. A. & SMITH, R. C. (2007), Climate change and the marine ecosystem of the western Antarctic Peninsula. *Philosophical Transactions of the Royal Society B-Biological Sciences*, 362, 149-166.
- MINCKS, S. L., SMITH, C. R. & DEMASTER, D. J. (2005), Persistence of labile organic matter and microbial biomass in Antarctic shelf sediments: evidence of a sediment 'food bank'. *Marine Ecology-Progress Series*, 300, 3-19.
- MONTES-HUGO, M., DONEY, S.C., DUCKLOW, H.W., FRASER, W., MARTINSON, D., STAMMERJOHN, S.E., SCHOFIELD, O. (2009), Recent Changes in Phytoplankton Communities Associated with Rapid Regional Climate Change Along the Western Antarctic Peninsula. *Science*, 323, 1470-1473.
- NEDWELL, D. B. (1999), Effect of low temperature on microbial growth: lowered affinity for substrates limits growth at low temperature. *Fems Microbiology Ecology*, 30, 101-111.
- SMITH, D. A. & KLINCK, J. M. (2002), Water properties on the west Antarctic Peninsula continental shelf: a model study of effects of surface fluxes and sea ice. *Deep-Sea Res. II* 49, 4863–4886.
- SMITH, C. R., MINCKS, S. & DEMASTER, D. J. (2006), A synthesis of benthic-pelagic coupling on the Antarctic shelf: Food banks, ecosystem inertia and global climate change. *Deep-Sea Research Part II-Topical Studies in Oceanography*, 53, 875-894.
- VAUGHAN, D. G. & DOAKE, C. S. M. (1996), Recent atmospheric warming and retreat of ice shelves on the Antarctic Peninsula. *Nature*, 379, 328–331.